Eur Biophys J (2006) 35: 431–438
DOI 10.1007/s00249-006-0050-1

ARTICLE

L. P. Cavalcanti · O. Konovalov · I. L. Torriani

Lipid model membranes for drug interaction study

Received: 26 October 2005 / Revised: 1 February 2006 / Accepted: 8 February 2006 / Published online: 6 April 2006

Abstract The present work shows a structural study on the process of incorporation of a hydrophobic drug, Ellipticine (ELPT), into lipid model membranes for drug targeting purpose. The ELPT is an alkaloid that showed an anti-proliferation activity against several types of tumor cells and against the HIV1 virus. We used the zwitterionic lipid dipalmitoyl phosphatidylcholine (DPPC) and four different anionic lipids: cardiolipin (CL), dipalmitoyl phosphatidic acid (DPPA), dipalmitoyl phosphatidylglycerol (DPPG) and dipalmitoyl phosphatidylserine (DPPS), both spread on a Langmuir monolayer and deposited on a solid substrate to mimic a model membrane and study the interaction with the drug ELPT. X-ray reflectivity results pointed toward an increase in drug loading efficiency up to 13.5% mol/mol of ELPT into mixed systems DPPC/CL. This increase in loading efficiency was also accompanied by a slight distortion in the stacking of the bilayers less evidenced after optimization of the molar ratio between the co-lipids. Grazing incidence X-ray diffraction measurements revealed an in-plane lattice distortion due to the presence of hydrocarbon chain backbone ordering in pure systems of DPPC doped with ELPT. The same was not observed in mixed membranes with DPPC/CL and DPPC/DPPA.

Keywords Lipid model membranes · Diffraction · Langmuir films

Introduction

The mesophases of polar lipid layers represent an efficient structural model for the study of biological membranes, as it was firstly proposed in the 1970s after the work of Bangham (1968). In the present work, we used the zwitterionic lipid dipalmitoyl phosphatidylcholine (DPPC) to build model membranes mixed with four different anionic lipids to characterize the optimum molar ratio for the encapsulation of the anti-cancer agent Ellipticine (ELPT)into the system looking forward to the drug delivery application.

The ELPT, originally isolated from the Ochrosia Elliptica Tree is a highly hydrophobic alkaloid and consists of a planar heterocyclic ring system with a maximum dimension of 10 Å (see Fig. 1). A precise mechanism of action has not yet been explained but it has been suggested that its antitumoral activity is due to intercalation between base pairs of helical nucleic acids (Kohn et al. 1975) and inhibition of DNA topoisomerase II activity (Singh et al. 1994). Although the antitumor specificity of this molecule is still under investigation (Stiborová et al. 2001), it was found that ELPT shows excellent antitumoral activity against experimental and human tumors when studied in vitro. Some derivatives were selected for pre-clinical studies and they inhibited the proliferation of serious metastasis processes caused by different types of leukemia, carcinoma, melanoma and sarcoma. It was also demonstrated that ELPT has an anti-HIV activity (Mathe et al. 1998). Despite of these great advantages, the literature showed that some clinical tests were discontinued because the drug appeared not to reach the desired site of action satisfactorily apparently due to its insolubility in aqueous media (Sainsbury 1990).

This was the context for trying the idea to use a liposome to wrap and transport such a hydrophobic drug, since it has a good solubility in alkane media. This procedure would present the advantage that side effect shield and targeting of the liposome could be used for enhancing the efficacy. For probing that, we used Langmuir lipid monolayers on the air/water interface and also multilamellar thin films on a solid substrate as model membranes to study the interaction with the drug ELPT. The studies of El Mashak et al. (1979) on the

L. P. Cavalcanti (✉) · O. Konovalov
European Synchrotron Radiation Facility (ESRF),
Grenoble Cedex, France
E-mail: cavalcanti@esrf.fr

I. L. Torriani
State University of Campinas/Synchrotron Light
National Laboratory (LNLS), Campinas, SP, Brazil

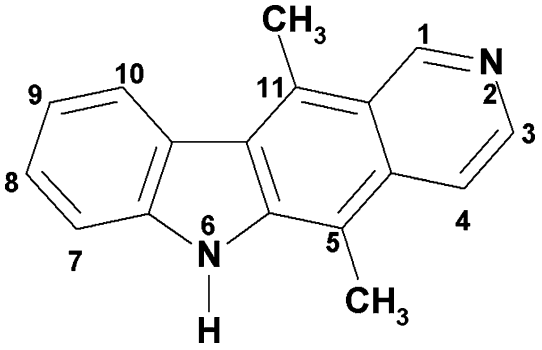

Fig. 1 Molecular structure of the anticancer agent Ellipticine (ELPT), C17H14N2 (5,11-dimethyl-6H-pyrido[4,3-b]carbazole), 246.3 g/mol

pressure-area isotherms of mixed systems lipid/ELPT have shown that the protonated form of the drug ELPT displays a very high affinity for anionic lipids, most notably for the cardiolipin (CL) and dipalmitoyl phosphatidic acid (DPPA). We then focused our attention on the model membranes made by DPPC mixed firstly with CL studied as multilamellar thin films, and then compared with model membranes made by DPPC mixed with DPPA, dipalmitoyl phosphatidylglycerol (DPPG) as dipalmitoyl phosphatidylserine (DPPS) as Langmuir monolayers.

Materials and methods

Two kinds of samples were prepared: multilamellar thin films and Langmuir monolayers more detailed in the following:

1. For the multilamellar-thin-film preparation, synthetic L-α-DPPC (Sigma) was first dissolved in chloroform and ELPT (Sigma) was dissolved in methanol. The two solutions were mixed together in appropriate proportions to achieve the desired molar fractions. The solvent of this mixture was evaporated under N_2 stream and the drug/lipid film was reconstituted with pure water and sonicated (L. P. Cavalcanti and I. L. Torriani, submitted). The resulting liposome suspensions were deposited on glass slides and dried in an environment of controlled humidity (relative humidity = 84%).

The dried multilamellar thin films were studied by X-ray reflectivity with a Cu-target rotating anode at State University of Campinas, Brazil. The X-ray beam energy at the sample was then 8.04 keV (Cu Kα $\lambda = 1.5418$ Å). The data acquisition was made in Bragg–Brentano geometry by a scintillate detector mounted on a step motor running with a typical step of 0.01° and 2 s acquisition time per point. The total exposure time per sample was about 50 min. The power of the source was set to 35 kV and 70 mA. No damage on the sample was observed with this setup.

2. For the Langmuir monolayer measurements, Synthetic L-α-DPPC (Sigma) was first dissolved in chloroform and ELPT (Sigma) was dissolved in methanol. The two solutions were mixed together in appropriate proportions to achieve the desired molar fractions. This mixture was spread at the air/water interface on a Langmuir trough. Residual surface pressure after solvent evaporation was below 0.5 mN/m. Then the surface pressure of the system was increased to the desired value through the movement of the barrier. Four different anionic lipids, CL, DPPA, DPPG and DPPS (Sigma) were studied combined with DPPC and loading the drug ELPT as a function of the area-pressure directly above the liquid expanded to liquid condensed phase transition.

Grazing incidence X-ray diffraction (GID) technique was used to study the in-plane order of lipid monolayers in the liquid condensed phase. In test experiments, we observed some degradation of the in-plane order due to radiation damage on the sample when the exposure time was more than 60 min. In order to reduce the effect of sample damage, the GID spectrum for each pressure was taken from a fresh sample area through a lateral trough displacement that was larger than the horizontal size of the beam, which was typically 0.5 mm. The total exposure time to obtain the two-dimensional map of diffraction was about 60 min per pressure for each sample. For this experiment, we worked with 16 bunches mode. The X-ray beam energy at the sample was 8.07 keV selected by a double crystal diamond monochromator from the first harmonic of three-undulator source at ID10B (Troika-II) beamline, European Synchrotron Radiation Facility (ESRF), France.

Theory on lattice parameter determination

A description of the structure of the Langmuir monolayer mesophases was proposed through the Landau theory by Kaganer and Loginov (1995). A compilation of the subject can be seen in Kaganer et al. (1995, 1999), and a detailed study in Fradin (1999). All possible structures were derived from the hexatic phase, the so-called LS, and it was considered to be unique. We repeat here some practical steps of the theory, which is reported in the cited papers above, for a quick consultation and a better understanding of data presented next.

Any two-dimensional lattice on the plane xy can be described by the centered oblique cell defined with the base vectors **a**, **b** and an angle γ between them. In practice, it is convenient to represent the oblique lattice as distorted orthogonal lattice with a distortion angle $\gamma' = \gamma - \pi/2$ as it is shown in Fig. 2. The base vectors **a** and **b** expressed in the orthogonal system of coordinates are:

$$\mathbf{a} = \begin{cases} -a\sin\gamma' \\ -a\cos\gamma' \\ 0 \end{cases} \qquad \mathbf{b} = \begin{cases} b \\ 0 \\ 0 \end{cases} \tag{1}$$

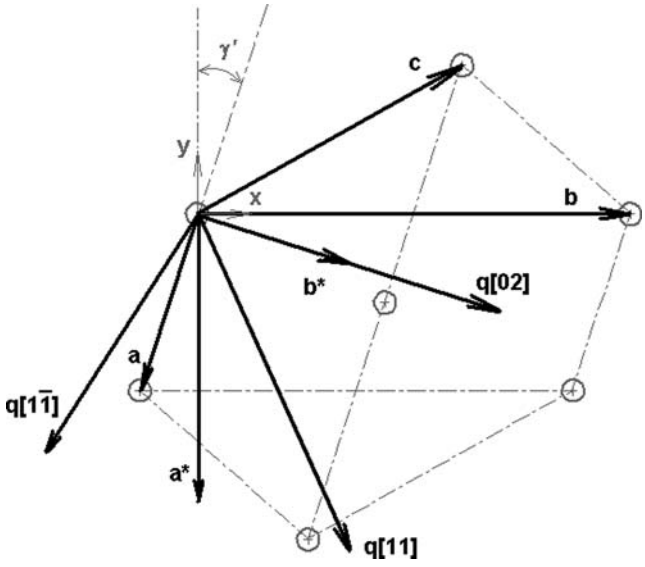

Fig. 2 General centered oblique cell defined by the base vectors **a** and **b** and the angle of distortion γ'. We can also consider the base vectors **a** and **c** for the primitive cell ($|c| = |b\text{-}a|/2$). Representation of the **q** vectors of the first three peaks appearing on the diffraction pattern

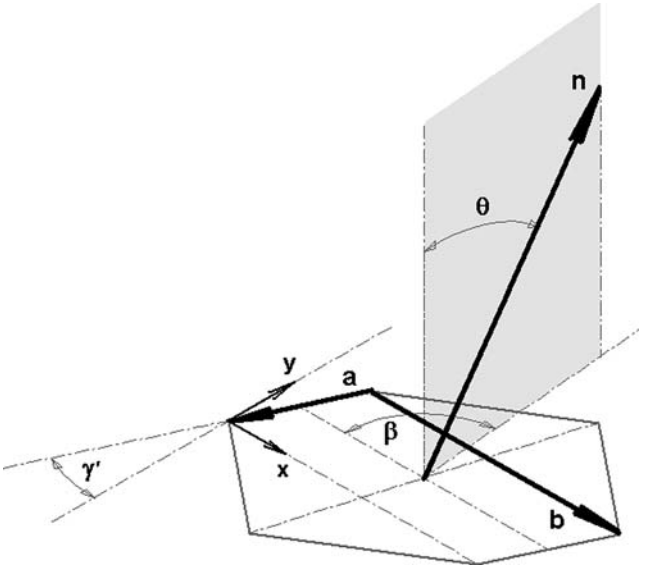

Fig. 3 Representation of the vector **n**: tilt direction of the molecules. The plane that contains n (in gray) is normal to the lattice plane

In this framework, the particular hexatic case is found when $b = \sqrt{3}a$ and $\gamma' = 0$. The Bragg peaks with Miller indices (hk) with an odd result for $h+k$ are absent for a hexatic structure. Then, the first three peaks appearing on the diffraction pattern will be [11], $[1\bar{1}]$ and [02]. Based on the scheme Fig. 2, we can calculate their values as follows:

$$\mathbf{q}[11] = \mathbf{a}^* + \mathbf{b}^* = \frac{2\pi}{ab\cos\gamma'} \begin{Bmatrix} a\cos\gamma' \\ -b - a\sin\gamma' \\ 0 \end{Bmatrix} \tag{2}$$

$$\mathbf{q}[1\bar{1}] = \mathbf{a}^* - \mathbf{b}^* = \frac{2\pi}{ab\cos\gamma} \begin{Bmatrix} -a\cos\gamma' \\ -b + a\sin\gamma' \\ 0 \end{Bmatrix} \tag{3}$$

$$\mathbf{q}[02] = 2\mathbf{b}^* = \frac{4\pi}{b} \begin{Bmatrix} 1 \\ -a\tan\gamma' \\ 0 \end{Bmatrix} \tag{4}$$

These are the values of q in the plane xy. We are not using the subscript xy for the sake of simplicity. From this, we can derive the lattice parameters as follows:

$$b = \frac{4\pi}{q[02]\cos\gamma'} \tag{5}$$

$$a = \frac{q[02]b}{\sqrt{2q[11]^2 + 2q[1\bar{1}]^2 - q[02]^2}} \tag{6}$$

$$\sin\gamma' = \frac{q[11]^2 - q[1\bar{1}]^2}{q[02]\sqrt{2q[11]^2 + 2q[1\bar{1}]^2 - q[02]^2}} \tag{7}$$

$$\gamma' = a\sin\left(\frac{q[11]^2 - q[1\bar{1}]^2}{q[02]\sqrt{2q[11]^2 + 2q[1\bar{1}]^2 - q[02]^2}}\right) \tag{8}$$

To describe the tilt of the molecules along the vector **n**, as seen in the scheme of Fig. 3, we can define two other parameters namely the collective tilt θ in respect to the plane normal and the azimuth tilt β, defined as the angle between the projection of vector **n** on the lattice plane and the base vector **b**.

$$\mathbf{n} = \begin{Bmatrix} -\sin\theta\cos\beta \\ \sin\theta\sin\beta \\ \cos\theta \end{Bmatrix} \tag{9}$$

If there is no tilt of the molecules ($\theta = 0$) then there will be no vertical components of $q[hk]$ as well. This is equivalent to say that the scalar product $q[hk]\cdot n$ is null for all peaks found in the two-dimensional structure. Applying this condition to each peak found above yields to the values of the vertical components in the case of $\theta \neq 0$, which we will label with a subscript **z** to distinguish from the parallel one.

$$q_z[11] = \frac{2\pi}{ab\cos\gamma'}\left[a\cos\gamma'\cos\beta + (b + a\sin\gamma')\sin\beta\right]\tan\theta \tag{10}$$

$$q_z[1\bar{1}] = \frac{2\pi}{ab\cos\gamma'}\left[-a\cos\gamma'\cos\beta + (b - a\sin\gamma')\sin\beta\right]\tan\theta \tag{11}$$

$$q_z[02] = \frac{4\pi}{b}\left[\cos\beta + \tan\gamma'\sin\beta\right]\tan\theta \tag{12}$$

These expressions then generate the ones to determine θ and β. The calculation that follows is simply isolating $\tan\theta$ from Eq. 12 and substituting it in the result of adding together Eqs. 10 and 11:

$$q_z[11] + q_z[1\bar{1}] = \frac{4\pi}{a\cos\gamma'}\sin\beta\tan\theta \tag{13}$$

$$\tan\theta = \frac{bq_z[02]}{4\pi[\cos\beta + \tan\gamma'\sin\beta]} \tag{14}$$

$$\frac{1}{\tan\beta} = \frac{b}{a\cos\gamma'}\frac{q_z[02]}{q_z[11] + q_z[1\bar{1}]} - \tan\gamma' \tag{15}$$

$$\beta = a\tan\left(1/\left(\frac{b}{a\cos\gamma'}\frac{q_z[02]}{q_z[11] + q_z[1\bar{1}]} - \tan\gamma'\right)\right) \tag{16}$$

$$\theta = a\tan\left(\frac{bq_z[02]}{4\pi[\cos\beta + \tan\gamma'\sin\beta]}\right) \tag{17}$$

In addition to these parameters, we can always think to describe the cell in terms of its distortion in relation to the hexatic phase LS. According to the work of Sirota et al. (1993), it is convenient to represent such a distortion of the general oblique cell, denoted by the letter *D*, by describing the behavior of the ellipse that circumscribes the oblique cell through the six nearest neighbors. The difference of the axis ratio of this ellipse from the unity is the order parameter of the distortion: $D = 1 - (A/B)$, where *A* and *B* are the semi-minor and semi-major axes, respectively. Converting to the present oblique cell nomenclature, we can use $D = 1 - (b/a\sqrt{3})$. By doing that, one can easily find that the distortion *D* goes to zero when the structure tends to the hexatic phase.

The work of Kaganer et al. (1995) describes in detail how to determine the magnitude and phase of the cell distortion, denoted by the lowercase letter *d*, in terms of the lattice parameters. The magnitude ξ is given by:

$$\xi = \sqrt{2}\frac{\sqrt{\left\langle (q^2 - \langle q^2\rangle)^2\right\rangle}}{\langle q^2\rangle}, \tag{18}$$

where the averages includes the values of q_{xy} (*q* parallel) for all three peaks. The phase of the distortion *d* is related to the azimuth ω of the lattice distortion. Here, we just present the expression that relates all the entities:

$$d = \xi\cos 2(\omega - \beta) \tag{19}$$

In the same work of Kaganer et al. (1995), the Landau theory is used to find that the quantity *d* should be linearly dependent on $\sin^2(\theta)$, where θ is the tilt of the molecules. The quantity *d* is then the distortion of the unit cell induced exclusively by the tilt of the molecule.

Results and discussion

The ELPT incorporated in phospholipid bilayers can crystallize beyond a critical concentration. Experiments with DPPC bilayers showed two different crystalline phases for samples saturated with ELPT: (1) The phase I appears above 5% mol/mol concentration of ELPT in relation to DPPC and the structure is the standard crystalline phase indexed after the work of Courseille et al. (1974), (2) The phase II appears above 2.2% ELPT

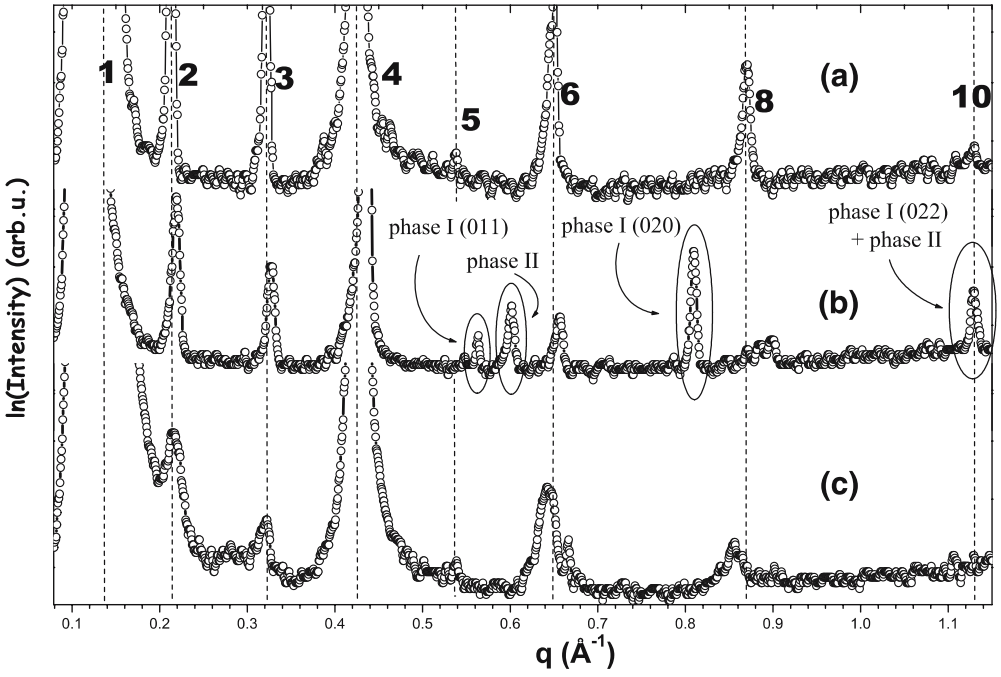

Fig. 4 The X-ray diffraction from multilamellar thin films of *(a)* pure DPPC results in several orders of *00l* reflections, numbered from 1 to 8 in the graph. Reflections of ELPT crystalline phases are observed in *(b)* DPPC/ELPT system but not in *(c)* DPPC/CL/ELPT one. The molar ratio between the parts are: *(a)* pure DPPC, *(b)* DPPC(6.6):ELPT(1), *(c)* DPPC(6.6):CL(0.8):ELPT(1). The molar ratio in *(c)* was set after the optimization described by Fig. 5

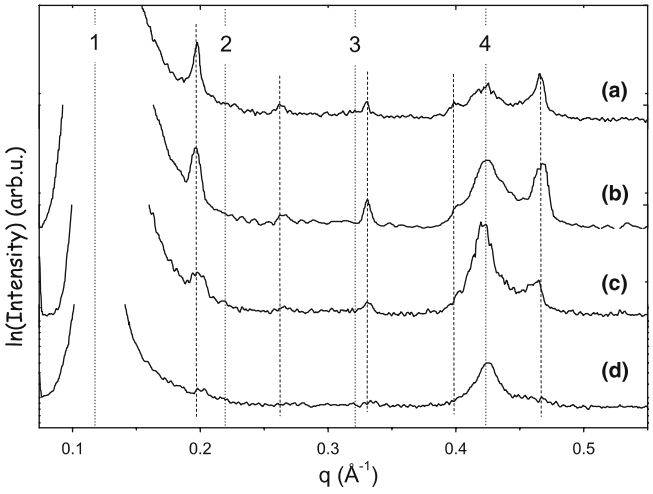

Fig. 5 The graph shows the diffraction pattern from four different molar ratio DPPC:CL: *(a)* 4.0:1, *(b)* 4.7:1, *(c)* 6.5:1, *(d)* 8.6:1. The *00l* reflections numbered from 1 to 4, come from the DPPC bilayer periodicity in the mixed system DPPC/CL. We can also observe a new set of *00l* reflections (*dashed lines*) with a small periodicity like a second phase of the system

in DPPC bilayers and this is a phase never identified before that is suggested to be a solvatomorph of ELPT induced by the mixture with the organic solvent methanol (L. P. Cavalcanti, in preparation).

The crystals and particles above a given size, are biologically toxic and cannot be inside an injectable pharmaceutical formulation. To monitor the occurrence of a crystalline phase of the drug we prepared samples of dried multilamellar thin films on a glass substrate made by DPPC with and without the drug ELPT and characterized by X-ray reflectivity. If no Bragg reflections from the crystalline phase of ELPT are observed, we can assume that the drug is totally dispersed in the lipid membrane in molecular form not presenting particle toxicity.

Following the results of the work of El Mashak et al.(1979), we introduced an anionic polar lipid as a co-lipid to prepare mixed model membranes for incorporation of ELPT. The first results came from the anionic lipid CL that showed an excellent increase in the solubility of ELPT in mixed bilayers DPPC/CL. The graphs of Fig. 4 show several orders of *00l* reflections from the multilamellar film. The fourth order of each system was considered to compare the periodicity values: (a) 58.7 Å, (b) 57.7 Å and (c) 58.7 Å. Comparing (a) and (b), one can also remark that inserting ELPT decreases slightly the membrane periodicity as observed in a previous work (Cavalcanti et al. 2005). Reflections of ELPT crystalline phases I and II were observed in (b) DPPC/ELPT system but not in (c) DPPC/CL/ELPT one. Both samples in (b) and (c) have the same molar ratio between ELPT and the total amount of lipid DPPC + CL, which is 13.5% mol/mol. It means six times the maximum dispersed ELPT that we had before with pure DPPC if considering the appearing of the solvatomorph crystals of ELPT after 2.2%. One should note that this value of 13.5% is not yet the maximum for the system DPPC/CL because higher concentrations were not tested. The increase in solubility of ELPT in the film DPPC/CL was, however, accompanied by a disorder in the stacking of the film bilayers. By comparing the *00l* reflections shown in Fig. 4, we observe that the higher orders are spoiled in *(b)*, *(c)* and we still have two phases in *(c)* that could be attributed to a side domain formation. The widths of the second, third and fourth-order diffraction peaks, taken as an example, are roughly twice larger when we add CL to the system. The values for the forth-peak widths are as follows: (0.0084 ± 0.0002) Å^{-1} for pure DPPC, (0.0079 ± 0.0002) Å^{-1} for DPPC/ELPT and (0.0180 ± 0.0004) Å^{-1} DPPC/CL/ELPT. Because of this, the molar ratio between DPPC and CL was studied in order to get the optimal compromise between the ordering of the bilayers and the solubility of ELPT in the system without formation of drug crystalline phase.

Figure 5 shows the result after testing four different molar ratios between DPPC and CL. The graph shows the *00l* reflections numbered from 1 to 4, that comes

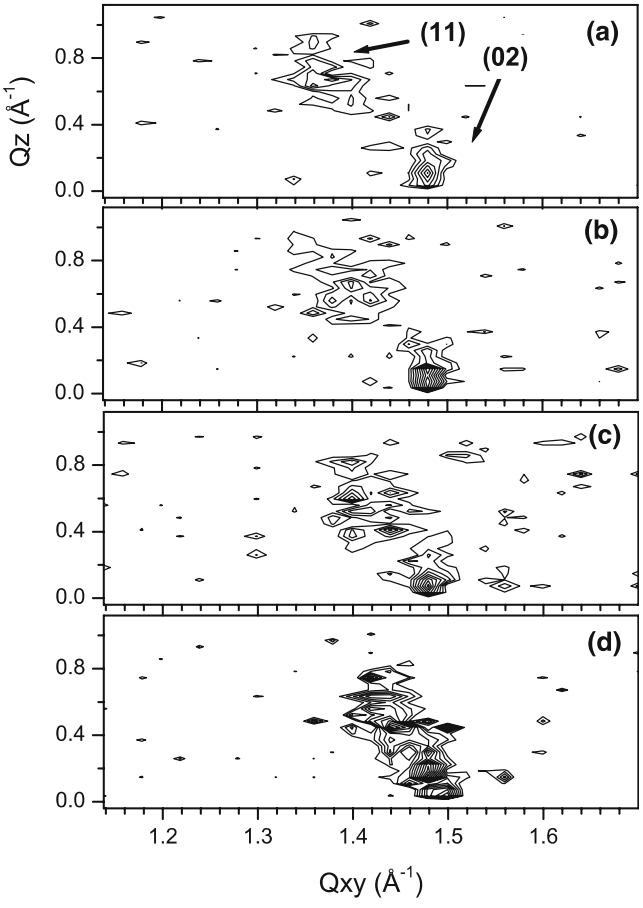

Fig. 6 GID mapping for DPPC/DPPA mixed membrane doped with 13.5% of ELPT. The corresponding surface pressures are *(a)* 15, *(b)* 20, *(c)* 25 and *(d)* 30 mN/m

from the DPPC matrix in the mixed system DPPC/CL, with a periodicity of (59.3 ± 0.3)Å and also a new set of *00l* reflections (dashed lines) with periodicity of (93.6 ± 0.7)Å. The difference of size and shape between CL and DPPC in the membrane must be causing a disorder in the stacking of the bilayers and formation of a separate phase or tilt domains. When the concentration of CL decreases the second phase tends to disappear as we see in Fig. 5c, d. The minimum tested molar ratio DPPC/CL 8.6:1 (Fig. 5d) was then considered to be the optimal for the present experiment and used as a reference to be compared to the other co-lipids studied further: DPPA, DPPG, and DPPS.

All of these three anionic co-lipids presented a high affinity for ELPT in the studies of El Mashak (1979). Some different characteristics between them and the molecule of CL are the stereo configuration and size of the headgroups, which should confer distinct membrane packing. We prepared Langmuir monolayers of mixed lipids DPPC/DPPA, DPPC/DPPG and DPPC/DPPS to be compared with DPPC/CL system. In all systems, we added the same amount of ELPT, which was 13.5% mol/mol (the quantity found to be totally dispersed in the DPPC/CL multilayer thin films). The mixed systems had then the following molar ratios: DPPC(6.6):CL(0.8): ELPT(1) and DPPC(5.96):DP(1.44): ELPT(1), where DP stand for DPPA, DPPG and DPPS. To control the stereo configuration of the membrane when mixed with co-lipids of different size and shape we considered the points discussed in the following. Since the CL has four alkyl chains, we took into account a factor 2 multiplying the number of molecules of the dialkyl co-lipids. The proportion between DPPC and CL was 8.25:1 (roughly the value found in Fig. 5*(d)*). Half of this value was taken for the systems DPPC/DPPA, DPPC/DPPG and DPPC/DPPS. In this way, we had an average of two molecules of DPPC for each hydrocarbon chain of any co-lipid. One should remark that, in this case, the net negative charges per drug molecule was not kept constant to be compared with the system DPPC/CL. The dialkyl systems DPPC/DPPA, DPPC/DPPG and DPPC/DPPS have 1.8 more net negative charges per drug molecule than the DPPC/CL one. This fact might influence on the packing of the membrane and also on the affinity for the drug in its protonated form where further studies could be done.

Table 1 Structural parameters of the Langmuir monolayers

Π (mN/m)	Lattice parameters						Collective tilt		Distortion	
	a (Å)	b (Å)	γ (°)	c (Å)	ϕ (°)	A (Å^2)	θ (°)	β (°)	ξ	D
Pure DPPC										
15	5.824	8.608	90	5.197	124.1	20.8	36.8	88.94	0.157	0.074
20	5.724	8.590	90	5.161	123.7	20.5	35.5	88.89	0.142	0.066
25	5.633	8.574	90	5.130	123.3	20.2	34.2	88.92	0.128	0.060
30	5.558	8.569	90	5.107	123.0	20.0	32.8	88.86	0.116	0.054
DPPC/ELPT										
15	5.812	8.606	90	5.192	124.0	20.7	37.4	88.89	0.155	0.072
20	5.730	8.581	90	5.159	123.7	20.4	37.0	89.02	0.145	0.068
25	5.645	8.581	90	5.136	123.3	20.2	35.7	89.06	0.130	0.061
30	5.567	8.566	90	5.108	123.0	20.0	35.1	88.96	0.118	0.055
DPPC/CL/ELPT										
15	5.623	8.582	90	5.130	123.2	20.2	36.1	88.92	0.126	0.059
20	5.508	8.559	90	5.089	122.8	19.8	32.7	88.77	0.108	0.050
25	5.403	8.539	90	5.052	122.3	19.5	30.3	88.75	0.091	0.042
30	5.323	8.523	90	5.024	122.0	19.2	27.4	88.59	0.078	0.036
DPPC/DPPA/ELPT										
15	5.405	8.539	90	5.053	122.3	19.5	30.2	88.55	0.092	0.042
20	5.276	8.516	90	5.009	121.8	19.1	27.2	88.58	0.070	0.032
25	5.209	8.498	90	4.984	121.5	18.9	24.1	88.50	0.060	0.027
30	5.118	8.475	90	4.950	121.1	18.6	20.6	88.06	0.045	0.020
DPPC/DPPG/ELPT										
15	5.615	8.579	90	5.127	123.2	20.2	34.6	88.77	0.125	0.058
20	5.532	8.571	90	5.100	122.8	19.9	32.9	88.87	0.111	0.052
25	5.435	8.544	90	5.063	122.5	19.6	30.9	88.87	0.097	0.045
30	5.362	8.527	90	5.037	122.2	19.4	29.1	88.69	0.085	0.039
DPPC/DPPS/ELPT										
15	5.640	8.596	90	5.140	123.3	20.3	34.7	88.86	0.127	0.059
20	5.516	8.567	90	5.095	122.8	19.9	32.7	88.77	0.109	0.050
25	5.422	8.546	90	5.060	122.4	19.6	30.9	88.78	0.094	0.043
30	5.332	8.526	90	5.028	122.0	19.3	27.8	88.62	0.080	0.036

All the samples, excepting the pure DPPC one, have an amount of 13.5% mol/mol concentration of ELPT in respect to the total amount of lipids. Π is the surface pressure of the Langmuir monolayer; a, b and γ are the lattice parameters of the centered cell; a, c and ϕ are the lattice parameters of the primitive cell; they can be determined by Eqs. 5, 6,and 8 with $\gamma = \gamma' + \pi/2$ and $|c| = |b - a|/2$; A is the area/chain; θ is the tilt of the molecule, Eq. 17; β is the azimuth of the tilt, Eq. 16; ξ is the magnitude of lattice distortion, Eq. 18; d is the lattice distortion, Eq. 19

For the characterization of the in-plane order, we used GID with the same geometry as described in the work of Konovalov et al. (2002). Figure 6 shows the GID mapping for the most interesting studied system made by DPPC/DPPA model membrane with incorporation of ELPT studied with four different surface pressures: 15, 20, 25 and 30 mN/m.

For all prepared mixed systems, we always observed two peaks identified as the degenerated reflection $[11] + [1\bar{1}]$ and the non-degenerated [02] reflection of a centered cell. The positions of the peaks changed as a function of pressure in the sense of increasing symmetry. The diffraction peak positions Qz and Qxy were taken in order to determine the lattice parameters of the centered cell a, b and γ. Table 1 shows also the parameters c and ϕ, where ϕ is the angle between a and c for the primitive cell.

Through the lattice parameters given in Table 1, we were able to determine the distortion of each system according Eq. 19 as a function of $\sin^2(\theta)$ for each surface pressure. Data was plotted in the graph of Fig. 7. They show a linear behavior, which indicates a good commonality of the structure. The extrapolation of the line in the limit of tilt $\theta = 0$ should brings us to a distortion $d = 0$ in the case of unit cell distortion exclusively due to the tilt of the molecules. In the cases other than that, we can have the contribution from the hydrocarbon-chain backbone plane ordering to the distortion of the unit cell. By the graphs of Fig. 7, we observe that the ordering in the backbone planes is contributing to the distortion of the pure DPPC system with and without ELPT (systems a and b). The same is not observed for the mixed model membranes prepared with (c) CL or (d) DPPA where the linear coefficient tends to zero and it is only slightly evidenced for the other anionic lipids (e) DPPG and (f) DPPS.

Summary and final remarks

An X-ray reflectivity study on ordered multilamellar thin films of DPPC and CL deposited on glass substrate confirmed that the addition of an anionic polar lipid as a co-lipid into model membranes increases the incorporation of the drug ELPT in its non-crystalline form. This could be explained by the fact that the anionic lipid can combine with the protonated form of ELPT. The

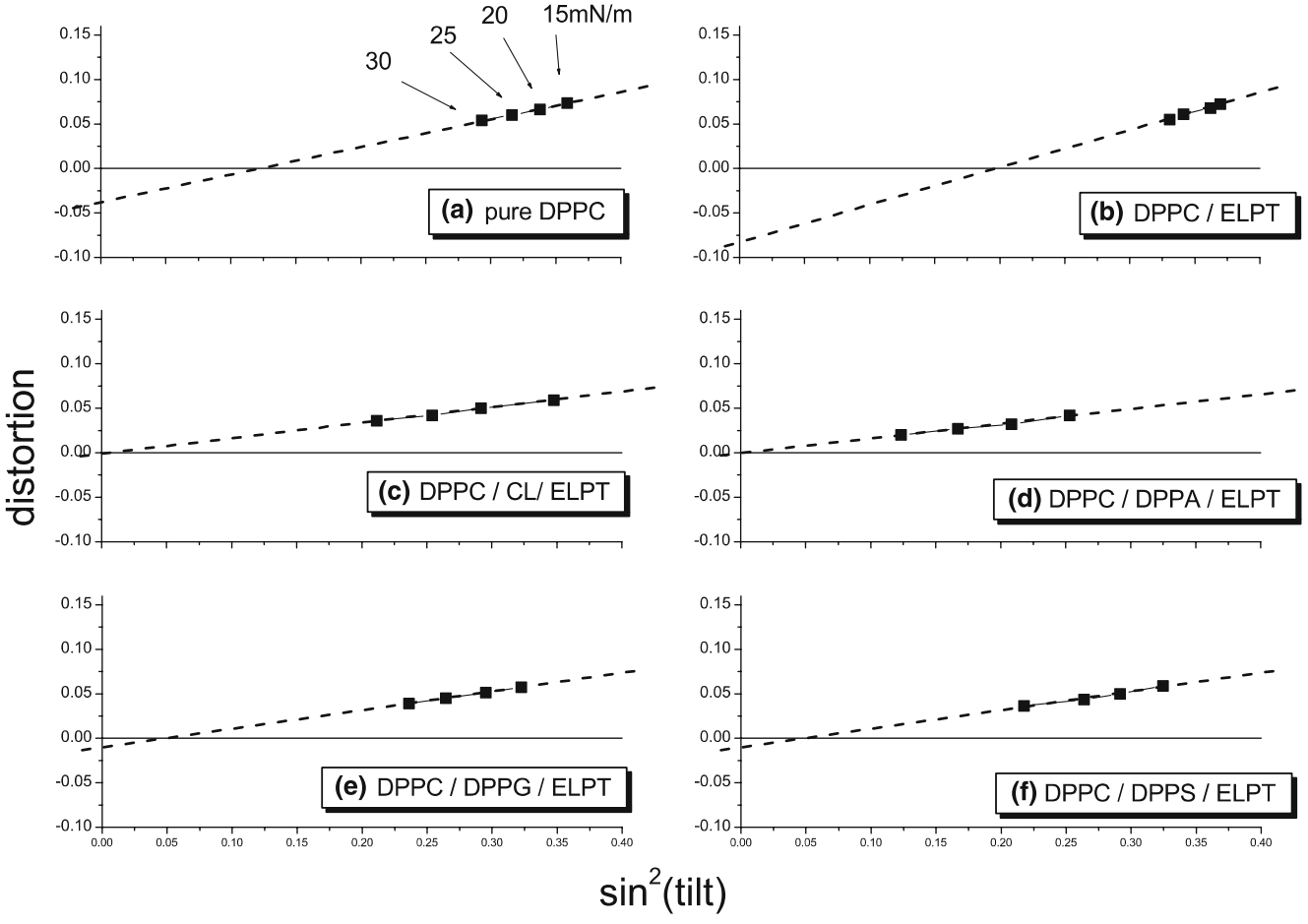

Fig. 7 The unit cell distortion is linearly dependent on $\sin^2(\theta)$. The *dashed line* is the linear regression for all different surface pressures extrapolated to the limit of tilt $\theta = 0$. The distortion due to the ordering of the backbone planes is observed for *(a)* and *(b)* where d#0 for tilt $= 0$; inexistent in *(c)* and *(d)* where the linear coefficient tends to zero and only slightly signed in *(e)* and *(f)*

nitrogen of position 2, shown in the molecular structure of ELPT in Fig. 1, may be protonated depending on the pH. In this case, further studies could be done as a function of the pH since it will change the offer of protonated form in the system.

The mixed membrane DPPC/CL can present some disordering of stacking and/or side domain formation compared with the pure DPPC system.

We looked for optimizing the molar ratio between DPPC and CL in mixed systems with a compromise on increasing the drug ELPT incorporation into the model membrane and having small effects of matrix disarray.

Studies on mixed model membranes made by DPPC and four different anionic lipids, CL, DPPA, DPPG and DPPS on Langmuir monolayers using GID have given further information about in-plane order of the lipid matrix. We observed an in-plane lattice distortion due to the presence of hydrocarbon chain backbone ordering in pure systems of DPPC doped with ELPT. The same was not observed in mixed membranes with DPPC/CL and DPPC/DPPA doped with the same amount of ELPT. The strong interaction between the anionic lipids and ELPT may promote a restructuring of the matrix.

The present work contributes essentially with results for controlling the presence of toxic crystals of ELPT in pharmaceutical formulations, a way to increase the loading efficiency of the carriers using anionic co-lipids and an alternative way to control the integrity of the carrier lipid matrix by studying the stacking ordering of multilayer thin films and the in-plane distortion of the Langmuir monolayers.

Acknowledgements The authors thank the European Synchrotron Radiation Facility (ESRF), France, for the use of beamtime at the Troika II beamline, the beamline staff, for the technical support and the CNPq Agency for funding part of this research in Brazil.

References

Bangham AD (1968) Membrane models with phospholipids. Prog Biophys Mol Biol 18:29–36

Cavalcanti LP et al (2005) Drug loading to lipid-based cationic nanoparticles. Nucl Instr Meth B 238:290–293

Courseille C et al (1974) Structure Cristalline et Moléculaire du Diméthyl-5,11 6H-Pyrido[4,3-b]carbazole (Ellipticine). Acta Cryst B30:2628–2631

El Mashak EM et al (1979) Interactions between ellipticine and some derivatives and phospholipids in model membranes. FEBS Lett 107:155–159

Fradin C (1999) These de doctorat, Universite Paris-6, France

Kaganer VM, Loginov EB (1995) Symmetry and phase-transitions in langmuir monolayers—the Landau theory. Phys Rev E 51:2237–2249

Kaganer VM et al (1995) Tilted phases of fatty acid monolayers. J Chem Phys 102:9412–9422

Kaganer VM et al (1999) Structure and phase transitions in Langmuir monolayers. Rev Mod Phys 71:779–819

Kohn K et al (1975) Intercalative binding of ellipticine to DNA. Cancer Res 35:71–76

Konovalov O et al (2002) Lipid discrimination in phospholipid monolayers by the antimicrobial frog skin peptide PGLa. A synchrotron X-ray grazing incidence and reflectivity study. Eur Biophys J 31: 428–437

Mathe G et al (1998) Viral and immunologic follow up of 4 to 9 years of AIDS treatments by quadruple combinations of virostatics including integrase inhibitors applied in short sequences differing by drug rotation'. Biomed Pharmacother 52:391–396

Sainsbury M (1990) Ellipticines. In: Wilman D (ed) The chemistry of antitumor agents. Chapman and Hall, New York, pp 410–435

Singh MP et al (1994) High-field NMR and restrained molecular modeling studies on a DNA heteroduplex containing a modified apurinic abasic site in the form of covalently linked 9-aminoellipticinet. Biochemistry 33:10271–10285

Sirota EB et al (1993) Rotator phases of the normal alkanes: an X-ray scattering study. J Chem Phys 98:5809–5824

Stiborová M et al (2001) The anticancer agent ellipticine on activation by cytochrome P450 forms covalent DNA adducts. Biochem Pharmac 62:1675–1684